IOPscience iopscience.iop.org

Home Search Collections Journals About Contact us My IOPscience

Antiferromagnetic quantum criticality induced by onset of superconductivity around upper critical field: non-Fermi liquid behavior of $CeCoIn_5$ at $H \simeq H_{c2}$

This article has been downloaded from IOPscience. Please scroll down to see the full text article.

2008 J. Phys.: Condens. Matter 20 325226

(http://iopscience.iop.org/0953-8984/20/32/325226)

View the table of contents for this issue, or go to the journal homepage for more

Download details:
IP Address: 129.252.86.83
The article was downloaded on 29/05/2010 at 13:49

Please note that terms and conditions apply.

J. Phys.: Condens. Matter **20** (2008) 325226 (7pp) doi:10.1088/0953-8984/20/32/325226

Antiferromagnetic quantum criticality induced by onset of superconductivity around upper critical field: non-Fermi liquid behavior of $CeCoIn_5$ at $H \simeq H_{c2}$

Yukinobu Fujimoto, Atsushi Tsuruta and Kazumasa Miyake

Division of Materials Physics, Department of Materials Engineering Science, Graduate School of Engineering Science, Osaka University, Toyonaka, Osaka 560-8531, Japan

E-mail: fujimoto@blade.mp.es.osaka-u.ac.jp

Received 6 February 2008, in final form 3 June 2008
Published 18 July 2008
Online at stacks.iop.org/JPhysCM/20/325226

Abstract

It is argued that the non-Fermi liquid behavior observed in $CeCoIn_5$ and its solid solution $CeCo(In, Sn)_5$ around the upper critical field H_{c2} can be understood as the antiferromagnetic (AF) quantum criticality induced by the critical fluctuations associated with an onset of the d-wave superconductivity with $B_{1g}(d_{x^2-y^2})$ or $B_{2g}(d_{xy})$ symmetry. A basic idea is that the effect of SC fluctuations on the mode-coupling term of the AF susceptibility works to promote the AF-order while those effect on the RPA term works to suppress the AF tendency. On the basis of this idea, the pinning of AF-QC around H_{c2} observed in $CeCo(In, Sn)_5$ can be qualitatively explained.

The recent discovery of non-Fermi liquid (NFL) behavior around the upper critical field $H_{c2}(0)$ in $CeCoIn_5$ (and its solid solution with In slightly substituted by Sn) has been attracting much attention [1–3]. When a variety of magnetic fields are applied at low temperatures, the relationship between the resistivity ρ and temperature T is given by the equation $\rho = \rho_0 + AT^2$ where the coefficient A of the T^2 term strongly depends on the strength of the magnetic field. When the magnetic field H is far larger than the critical field H_{QCP} (denoted as H^* in [1]), the coefficient A is technically independent of the magnetic field H and the system is still in a paramagnetic state, meaning that AF-ordering does not appear. There is a tendency that as the magnetic field H becomes small and approaches H_{QCP}, the coefficient A becomes large and diverges. The H dependence of A at $T = 0$ K is experimentally determined as $A \propto (H - H_{QCP})^{\alpha}$ with parameters $H_{QCP} = 5.1 \pm 0.2$ T and $\alpha = -1.37 \pm 0.1$. We can easily see that it exhibits quantum critical behavior at $H = H_{QCP}$ where the coefficient A diverges. The FL theory tells us that the divergence of the coefficient A means the gigantic enhancement of the effective mass of a renormalized electron. This mass enhancement reflects the emergence of antiferromagnetism at $T = 0$ K and $H = H_{QCP}$, in other words field-induced AF quantum criticality. What is singular and intriguing is that H_{QCP} is close to $H_{c2}(0)$.

Moreover, what is surprisingly novel is that the NFL behavior, the emergence of AF-QC, is pinned at $H \simeq H_{c2}(0)$ even though $H_{c2}(0)$ is considerably altered by the substitution of In by Sn, e.g; $H_{c2}(0)$ is reduced to about a half by the substitution of In by Sn of about 10% [3]. It means that the pinning of AF-QC around $H_{c2}(0)$ invariably occurs regardless of the substitution of In by Sn. This gives us the validation of our opinion that the pinning of AF-QC around H_{c2} is not accidental but essential, thus implying that there is a physical rationale behind it. Furthermore, when we pay attention to the generally conceived fact that the superconducting (SC) fluctuations are remarkable at the boundary between the SC and normal states, this suggests that the NFL behavior, the emergence of AF-QC, be triggered by the one-dimensional (1d) nature of the superconducting (SC) fluctuations under an applied magnetic field $H \simeq H_{c2}(0)$.

The purpose of this paper is to demonstrate that the case mentioned above proves to hold true, by analyzing the effect of SC fluctuations on the antiferromagnetic (AF) susceptibility in the framework of the mode-coupling theory for the onset of AF-ordering. A fundamental idea is that

 © 2008 IOP Publishing Ltd Printed in the UK

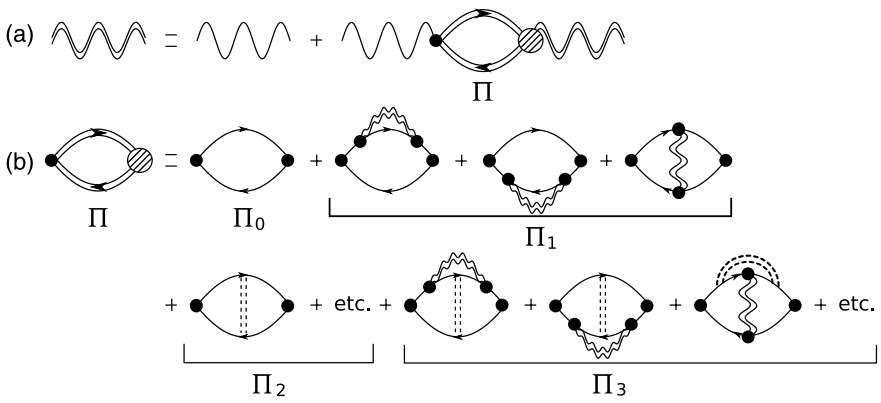

Figure 1. Feynman diagram for the mode-coupling theory with SC fluctuations. The double wavy line represents χ_s, the single wavy line χ_{so}, the single solid line Green's function for the itinerant fermions G, the double dashed line the SC fluctuations D, and the filled circle the coupling constant g. Π represents the polarization function of itinerant fermions.

the mode-coupling terms of AF fluctuations, which negatively contribute to AF-ordering, are suppressed by SC fluctuations, thus leading to the stabilization of the AF-ordering. In the low temperature limit $T \to 0$, $CeCoIn_5$ does not exhibit AF-ordering, but exhibits d-wave superconductivity. However, it is believed to be located close to the AF quantum critical point (QCP) [1, 4, 5]. This is also reinforced by a phase diagram confirmed by a series of compounds of solid solutions $Ce(Co_xRh_{1-x})In_5$, suggesting that rather strong AF fluctuations prevail in $CeCoIn_5$ [6]. Therefore, from the standard spin-fluctuation theory of itinerant magnetism [7], it is understood that the mode-coupling terms barely suppress the occurrence of AF-ordering in $CeCoIn_5$. Then, it is expected that the SC fluctuations are crucial in giving rise to the AF-QCP, which is located at the boundary between the SC and normal states.

The reason why the SC fluctuations are so crucial is that they become one-dimensional near $H \simeq H_{c2}(0)$ due to the Landau quantization of the Cooper-pair wavefunction. $CeCoIn_5$ is a quasi-two-dimensional d-wave superconductor and its SC fluctuations are three-dimensional (3d) without an applied magnetic field. However, an applied magnetic field perpendicular to the basal plane of $CeCoIn_5$ removes the freedom of its SC fluctuations along the x and y axes since the Landau quantization of the Cooper-pair wavefunction makes $CeCoIn_5$ to have discrete energy levels of x and y components and a continuous energy level of z component, thus meaning that the SC fluctuations become one-dimensional along the z-axis. Moreover, the mode-coupling theory has been successful so far in offering us an elaborate description of how a variety of AF-QCPs emerge [8]. Therefore, we will try to explain the appearance of the novel AF-QCP on the basis of mode-coupling theory with SC fluctuations.

The dynamical susceptibility $\chi_s(\mathbf{Q}+\mathbf{q}, i\omega_m)$ is expressed in the mode-coupling theory as [9–11]

$$\chi_s^{-1}(\mathbf{Q}+\mathbf{q}, i\omega_m) = \chi_{s0}^{-1}(\mathbf{Q}+\mathbf{q}, i\omega_m) - \Pi(\mathbf{Q}+\mathbf{q}, i\omega_m), \quad (1)$$

$$\mathbf{Q} \simeq (\pi/a, \pi/a, 0), \quad (2)$$

where χ_{s0} is the dynamical susceptibility of the localized spin fluctuations without the coupling with itinerant fermions, $\mathbf{Q}$ is AF-ordering vector, and a is the lattice constant in the basal plane perpendicular to the c-axis. The localized spin fluctuation χ_{s0} is coupled with the itinerant-fermion polarization Π as shown in equation (1) and figure 1. The polarization function $\Pi(\mathbf{Q}+\mathbf{q}, i\omega_m)$ plays a crucial role in giving rise to the AF-QCP and is given as follows:

$$\Pi(\mathbf{Q}+\mathbf{q}, i\omega_m) = \Pi_0(\mathbf{Q}+\mathbf{q}, i\omega_m) + \Pi_1(\mathbf{Q}+\mathbf{q}, i\omega_m) + \Pi_2(\mathbf{Q}+\mathbf{q}, i\omega_m) + \Pi_3(\mathbf{Q}+\mathbf{q}, i\omega_m), \quad (3)$$

where Π_0 and Π_1 are defined as

$$\Pi_0(\mathbf{Q}+\mathbf{q}, i\omega_m) \equiv -g^2 T \sum_n \sum_{\mathbf{p}} G(\mathbf{p}, i\epsilon_n) G \times (\mathbf{p}+\mathbf{Q}+\mathbf{q}, i\epsilon_n + i\omega_m), \quad (4)$$

$$\Pi_1(\mathbf{Q}+\mathbf{q}, i\omega_m) \equiv -g^4 T \sum_{m'} \sum_{\mathbf{q}'} [6G_4^{(s)} - G_4^{(v)}] \times \chi_s(\mathbf{Q}+\mathbf{q}', i\omega_{m'}), \quad (5)$$

where $G(\mathbf{p}, i\epsilon_n)$ is Green's function for the itinerant fermion, and g is the coupling constant between localized spin fluctuations and itinerant fermions, and related to the fermion coherence temperature (or the effective Fermi energy) E_F^* by $zg \sim E_F^*$, with z being the renormalization amplitude [9]. $G_4^{(s)}$ and $G_4^{(v)}$ are defined as

$$G_4^{(s)} = T \sum_n \sum_{\mathbf{p}} G(\mathbf{p}, i\epsilon_n) G^2(\mathbf{p}+\mathbf{Q}+\mathbf{q}, i\epsilon_n + i\omega_m) \times G(\mathbf{p}+\mathbf{q}-\mathbf{q}', i\epsilon_n + i\omega_m - i\omega_{m'}), \quad (6)$$

$$G_4^{(v)} = T \sum_n \sum_{\mathbf{p}} G(\mathbf{p}, i\epsilon_n) G(\mathbf{p}+\mathbf{Q}+\mathbf{q}, i\epsilon_n + i\omega_m) \times G(\mathbf{p}-\mathbf{Q}-\mathbf{q}', i\epsilon_n - i\omega_{m'}) \times G(\mathbf{p}+\mathbf{q}-\mathbf{q}', i\epsilon_n + i\omega_m - i\omega_{m'}), \quad (7)$$

where $G_4^{(s)}$ represents each of the two left diagrams of Π_1, and $G_4^{(v)}$ represents the last diagram of Π_1 as shown in figure 1. Using equations (1), (3), and (4), we expand the spin-fluctuation propagators $\chi_s(\mathbf{Q}+\mathbf{q}, i\omega_m)$ and $\chi_{RPA}(\mathbf{Q}+\mathbf{q}, i\omega_m)$ with respect to $\mathbf{q}$ and ω_m in the vicinity of AF-order vector $\mathbf{Q}$ as

$$\chi_s(\mathbf{Q}+\mathbf{q}, i\omega_m) = \frac{N_F^*}{r + A\mathbf{q}^2 + c|\omega_m|}, \quad (8)$$

$$\chi_{\rm RPA}(\mathbf{Q}+\mathbf{q}, {\rm i}\omega_m) = \chi_{s0}^{-1}(\mathbf{Q}+\mathbf{q}, {\rm i}\omega_m) - \Pi_0(\mathbf{Q}+\mathbf{q}, {\rm i}\omega_m) = \frac{N_{\rm F}^*}{r_0 + A\mathbf{q}^2 + c|\omega_m|}, \quad (9)$$

where $N_{\rm F}^*$ is the density of states (DOS) of quasiparticles at the Fermi energy. Parameters r and r_0 denote the distances from the AF-QCP in the mode-coupling theory and random phase approximation (RPA), respectively. The relations $r > 0$ and $r = 0$ correspond to the paramagnetic state and the AF-QCP, respectively.

The polarization function Π can be separated into two parts as shown in figure 1. One consists of the polarization functions Π_0 and Π_1 without the effect of the SC fluctuations, both of which are conventionally involved into the mode-coupling theory. The other consists of the polarization functions Π_2 and Π_3 with the effect of the SC fluctuations. The polarization Π_1 includes the dynamical susceptibility χ_s in a self-consistent fashion. While Π_0 associated with RPA promotes the AF-QCP, Π_1 suppresses it. Near the AF-QCP, the negative contribution of Π_1 to the appearance of the AF-QCP barely precedes the positive one of $\chi_{\rm RPA}^{-1} (= \chi_{\rm so}^{-1} - \Pi_0)$ to it. The state without the effect of the SC fluctuations as shown in figure 1(a) is considered to be in such a situation where the system is in the proximity of the AF-QCP [4, 5].

Now, we take into account the fact that the SC fluctuations are remarkable in the vicinity of the upper critical field $H_{\rm c2}(0) = H_{\rm QCP}$ at $T = 0$ K. Therefore, we include the effect of the SC fluctuations into the polarization functions Π_0 and Π_1 as shown in figure 1(b). In the vicinity of $H_{\rm c2}(0)$, $CeCoIn_5$ is in the FFLO state where a Cooper-pairing state with a finite center-of-mass momentum $\mathbf{q_0}$ is realized due to the Pauli paramagnetic effect [12–14]. Considering the FFLO state, the resultant effective Hamiltonian is given by

$$H = \sum_{\mathbf{p},\sigma} \xi(\mathbf{p}) c_{\mathbf{p},\sigma}^{+} c_{\mathbf{p},\sigma} + \sum_{\mathbf{p},\mathbf{p}'} V_{\mathbf{p},\mathbf{p}'} c_{\mathbf{p}+\mathbf{q_0}/2,\uparrow}^{+} c_{-\mathbf{p}+\mathbf{q_0}/2,\downarrow}^{+} c_{-\mathbf{p}'+\mathbf{q_0}/2,\downarrow} c_{\mathbf{p}'+\mathbf{q_0}/2,\uparrow}, \quad (10)$$

where $\xi(\mathbf{p})$ is the energy dispersion of quasiparticles with momentum $\mathbf{p}$ measured relative to the Fermi energy, $\mathbf{q}_0$ is the center-of-mass momentum of a Cooper-pair, and $V_{\mathbf{p},\mathbf{p}'}$ is the Cooper-pairing potential. Since $CeCoIn_5$ is in the clean limit [15], the single-particle Green's function for the FFLO state is given by

$$G(\mathbf{p}, \varepsilon_n) = [{\rm i}\varepsilon_n - \xi(\mathbf{p}) + \sigma^z \mu_B H]^{-1}, \quad (11)$$

where $\varepsilon_n = (2n+1)\pi T$ is a fermion Matsubara frequency and σ^z is the z component of the Pauli matrices.

The phase transition from the normal state to the FFLO state in the vicinity of the absolute zero temperature is known to be a first-order one [16, 17]. However, the phase transition around $H \sim H_{\rm c2}(T \ll T_{\rm c0})$ can be regarded as a weakly first-order one because we are interested in the global behavior of the SC and AF fluctuations as T approaches zero from the region of $T \sim T_{\rm c0}$ with $T_{\rm c0}$ being the superconducting transition temperature without magnetic field. Namely, as far as the gross T-dependence of the AF susceptibility $\chi_s(Q)$ is concerned, the difference in the type of the SC transition at $H \sim H_{\rm c2}(T \ll T_{\rm c0})$, that is to say, whether its transition is a weakly first-order one or second-order one, is not expected to give an essential influence on the gross T-dependence of the AF susceptibility $\chi_s(Q)$ except in the narrow low temperature region $T \ll T_{\rm c0}$. As a consequence, it gives us a validation of the derivation of the SC fluctuations around $H = H_{\rm c2}(0) (T \ll T_{\rm c0})$ as T decreases from $T_{\rm c0}$ to $T = 0$ on the basis of the second-order transition.

After straightforward but rather lengthy calculations based on equations (10) and (11), the SC fluctuation propagator D for the FFLO state is obtained as [18]

$$D(\mathbf{q}, {\rm i}\omega_m) = \frac{1}{N_{\rm F}^*}\left[\ln\left(\frac{T}{T_{\rm c0}}\right) + \int \frac{{\rm d}^3\hat{\mathbf{p}}}{4\pi}\psi\left(\frac{1}{2} + \frac{|\omega_m|}{4\pi T} + {\rm i}\frac{2\mu_B H + \langle v_{\mathbf{p}} \cdot (\mathbf{q}_0 + \mathbf{q})\rangle_{\rm FS}}{4\pi T}\right) - \psi\left(\frac{1}{2}\right)\right]^{-1}, \quad (12)$$

where $T_{\rm c0}$ is the superconducting transition temperature without the magnetic field, ψ is the digamma function, $v_{\mathbf{p}}$ is the velocity of the quasiparticle, and $\langle\cdots\rangle_{\rm FS}$ denotes the averaging over the Fermi surface. Furthermore, $CeCoIn_5$ is a type-II superconductor in which the orbital effect is to be considered [12]. Then, the eigenvalue of $\mathbf{q}^2$ is quantized as

$$\mathbf{q}^2 = \left(n + \frac{1}{2}\right)\frac{4eH}{c} + q_z^2, \qquad (n = 0, 1, 2, \ldots), \quad (13)$$

where H is the magnetic field, and q_z is the z component of the wavevector $\mathbf{q}$ of the SC fluctuations. Performing the summation of $D(\mathbf{q}, {\rm i}\omega_m)$ over $\mathbf{q}$ and ω_m with the use of equations (12) and (13) (with $n = 0$), we obtain in the low temperature limit

$$F_{\rm SC} \equiv T\sum_{\mathbf{q}}\sum_{{\rm i}\omega_m} D(\mathbf{q}, {\rm i}\omega_m)/E_{\rm F}^{*2} \simeq \gamma(m^*/m)^{1/2} - \delta(m^*/m)T, \quad (14)$$

where m is the mass of a bare electron, m^* is the effective mass of quasiparticles, and $E_{\rm F}^* \equiv \hbar^2 k_{\rm F}^2/2m^*$ is the renormalized Fermi energy. It is noted that the $\mathbf{q}$-dependence of the SC fluctuations near the superconducting transition temperature is one-dimensionally parameterized by q_z due to the Landau quantization (13), giving rise to an enhanced fluctuation effect. We can see from equation (14) that at low temperatures, the sum of the SC fluctuations does not diverge but has a peak with a cusp structure around $T = 0$ K and exhibits a linear decrease with temperature, which is shown in figure 2.

The Feynman diagrams for Π_2 (correction to Π_0 by the SC fluctuations) are shown in figure 3. Those for $\Pi_3^{(1)}$ and $\Pi_3^{(2)}$ (correction to Π_1 by the SC fluctuations), where $\Pi_3^{(1)}$ is a type of Green's function correction to the polarization function and $\Pi_3^{(2)}$ is that of the vertex correction to the polarization function, are shown in figures 4 and 5, respectively. Owing to the contribution of the SC fluctuations given by equation (14), the signs of Π_2 and Π_3 ($\equiv \Pi_3^{(1)} + \Pi_3^{(2)}$) are opposite to those of Π_0 and Π_1, respectively. Namely, while Π_0 promotes the appearance of the AF-QCP, Π_2 suppresses it. Similarly, while Π_1 suppresses the appearance of the AF-QCP, Π_3 promotes it. Here, we neglect Π_2, since $|\Pi_2|/|\Pi_3| \ll 1$ as we discuss below.

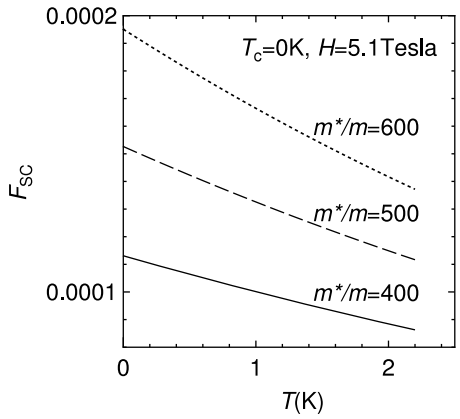

Figure 2. F_{SC} versus temperature with F_{SC} being defined by equation (14).

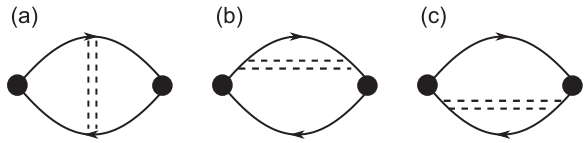

Figure 3. Feynman diagrams for the polarization function Π_2. The single solid line represents the Green's function of the itinerant fermions G, the double dashed line the SC fluctuations D, and the filled circle the coupling constant g.

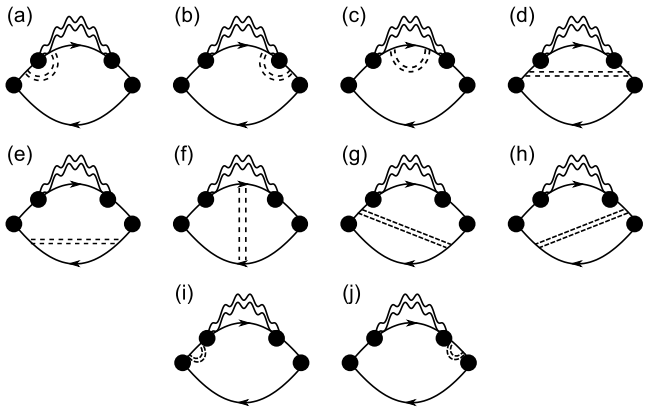

Figure 4. Feynman diagrams for the polarization function $\Pi_3^{(1)}$. The double wavy line represents χ_s, the single solid line the Green's function of the itinerant fermions G, the double dashed line the SC fluctuations D, and the filled circle the coupling constant g. In addition to these diagrams, there exist other longitudinally symmetrical Feynman diagrams, in which χ_s is situated at the bottom.

Thus, setting $\mathbf{q} = 0$ and $\omega_m = 0$ in equations (1), (3)–(5), and (9), we obtain

$$\chi_s^{-1}(\mathbf{Q}, 0) \simeq \{\chi_{\mathrm{RPA}}^{-1}(\mathbf{Q}, 0) - \Pi_1(\mathbf{Q}, 0)\} - \Pi_3(\mathbf{Q}, 0). \quad (15)$$

Let us for convenience introduce the following parameters in the conventional manner of the mode-coupling theory [7]:

$$y^* = \left\{\chi_{\mathrm{RPA}}^{-1}(\mathbf{Q}, 0) - \Pi_1(\mathbf{Q}, 0)\right\} / (Aq_{\mathrm{B}}^2/N_{\mathrm{F}}^*), \quad (16)$$

$$y = \chi_s^{-1}(\mathbf{Q}, 0)/(Aq_{\mathrm{B}}^2/N_{\mathrm{F}}^*), \quad (17)$$

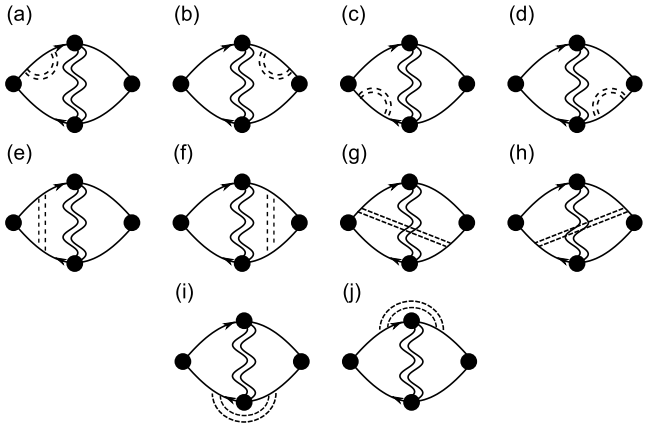

Figure 5. Feynman diagrams for the polarization function $\Pi_3^{(2)}$. The double wavy line represents χ_s, the single solid line the Green's function of the itinerant fermions G, the double dashed line the SC fluctuations D, and the filled circle the coupling constant g.

$$\Pi_3(\mathbf{Q}, 0)^* = \Pi_3(\mathbf{Q}, 0)/(Aq_{\mathrm{B}}^2/N_{\mathrm{F}}^*), \quad (18)$$

where q_{B} is the effective zone boundary wavenumber. Then, equation (15) is expressed as

$$y \simeq y^* - \Pi_3^*(\mathbf{Q}, 0) = \left\{y^*/|\Pi_1(\mathbf{Q}, 0)| - \frac{\Pi_3(\mathbf{Q}, 0)/|\Pi_1(\mathbf{Q}, 0)|}{(Aq_{\mathrm{B}}^2/N_{\mathrm{F}}^*)}\right\} |\Pi_1(\mathbf{Q}, 0)|, \quad (19)$$

where y^* corresponds to the deviation from the AF-QCP without the effect of the SC fluctuations and y corresponds to the deviation including their effect. The temperature dependence of y for 3d-AF is given by [8, 9, 19]

$$y = y_0 + \frac{3}{2} y_1 t \int_0^{x_c} \mathrm{d}x x^2 \left\{\ln u - \frac{1}{2u} - \psi(u)\right\}, \quad (20)$$

with

$$y_0 \equiv y \quad \text{at } T = 0 \text{ K}, \qquad x \equiv q/q_{\mathrm{B}}, \qquad x_c \equiv q_c/q_{\mathrm{B}},$$
$$u \equiv (y + x^2/t), \qquad t \equiv T/T_0, \qquad T_0 \equiv Aq_{\mathrm{B}}^2/2\pi C, \quad (21)$$

where q_c is the cut-off wavenumber and t is the dimensionless reduced temperature. Using the interpolation formula with high accuracy

$$\ln u - \frac{1}{2u} - \psi(u) \simeq \frac{1}{2u(1 + 6u)}, \quad (22)$$

equation (20) is reduced to

$$y \simeq y_0 + \frac{3}{2} y_1 t \int_0^{x_c} \mathrm{d}x \left\{\frac{x^2}{2(x^2 + y)} - \frac{x^2}{2(x^2 + y) + t/3}\right\}. \quad (23)$$

If the AF-ordering occurs, setting $y = 0$ and $t = t_{\mathrm{N}}$ in equation (23), the Néel temperature T_{N} is given by

$$0 \simeq y_0 + \frac{3}{2} y_1 t_{\mathrm{N}} \int_0^{x_c} \mathrm{d}x \left\{\frac{1}{2} - \frac{x^2}{2x^2 + t_{\mathrm{N}}/3}\right\}, \quad (24)$$

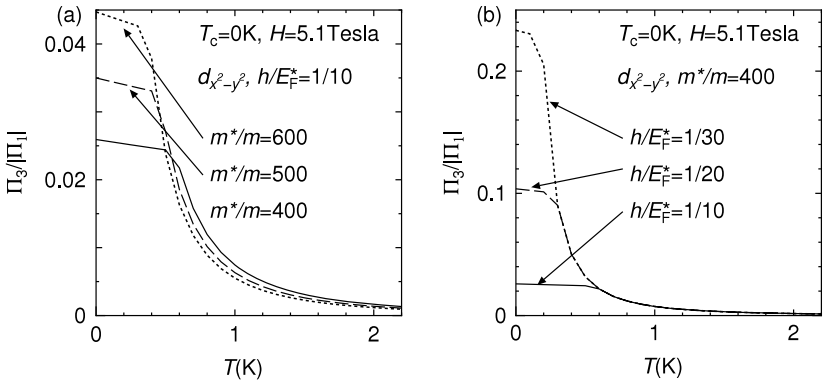

Figure 6. Temperature dependence of $\Pi_3(\mathbf{Q},0)/|\Pi_1(\mathbf{Q},0)|$ considering the SC fluctuations (a) for $m^*/m = 400, 500, 600$ with $h/E_F^* = 0.1$ and (b) for $h/E_F^* = 1/10, 1/20, 1/30$ with $m^*/m = 400$.

where $t_N = T_N/T_0$ is the dimensionless reduced Néel temperature. Here, the condition $y_0 = 0$ represents the AF-QCP. The coefficient $\Pi_3(\mathbf{Q},0)/|\Pi_1(\mathbf{Q},0)|$ included in the second term in the bracket $\{\cdots\}$ of the right-hand side of equation (19) is positive and exhibits a monotonous increase with decreasing temperature as shown in figure 2, thus promoting the AF-QCP. Using equation (14) and collecting the terms shown in figures 3–5, we obtain, in the low temperature limit,

$$\Pi_3(\mathbf{Q},0)/|\Pi_1(\mathbf{Q},0)| = \frac{93\zeta(5)}{112\pi^2\zeta(3)} \times [\gamma(m^*/m)^{1/2} - \delta(m^*/m)T]\left[\frac{E_F^*}{\max(T,h/2\pi)}\right]^2 \times \begin{cases} 46/5(\mathrm{d}_{xy}) \\ 4/5\ (\mathrm{d}_{x^2-y^2}), \end{cases} \tag{25}$$

$$\Pi_2(\mathbf{Q},0)/\Pi_0(\mathbf{Q},0) = \frac{7\zeta(3)}{8\pi^2} \times [\gamma(m^*/m)^{1/2} - \delta(m^*/m)T]\left[\frac{E_F^*}{\max(T,h/2\pi)}\right]^2 \times \begin{cases} -3(\mathrm{d}_{xy}) \\ -1(\mathrm{d}_{x^2-y^2}), \end{cases} \tag{26}$$

$$|\Pi_1(\mathbf{Q},0)|/\Pi_0(\mathbf{Q},0) \sim \left[\frac{zg}{\max(T,h/2\pi)}\right]^2 \times \ln\frac{E_F^*}{\max(T,h/2\pi)} \gg 1, \tag{27}$$

where h is the energy scale parameterizing the deviation from the perfect nesting [9]. Using equations (25)–(27), we obtain

$$|\Pi_2(\mathbf{Q},0)|/|\Pi_3(\mathbf{Q},0)| \sim |\Pi_0(\mathbf{Q},0)|/|\Pi_1(\mathbf{Q},0)| \sim \frac{[\max(T,h/2\pi)]^2}{E_F^{*2}\ln\frac{E_F^*}{\max(T,h/2\pi)}} \ll 1, \tag{28}$$

where $zg \sim E_F^*$ has been used. The factor $[\gamma(m^*/m)^{1/2} - \delta(m^*/m)T]$ on the right-hand side of equation (25) is due to the SC fluctuations on the right-hand side of equation (14). On the other hand, the factor $[E_F^*/\max(T,h/2\pi)]^2$ on the right-hand side of equation (25) depends on both the temperature T and energy scale parameterizing the deviation from the perfect nesting h. Therefore, in a region where $T < h/2\pi$, $\Pi_3/|\Pi_1|$ is dominated by the former factor and it represents the T-linear increase with decreasing temperature. However, in a region where $T > h/2\pi$, $\Pi_3/|\Pi_1|$ is dominated by the latter factor and it represents the inverse-T quadratic increase with decreasing temperature.

$CeCoIn_5$ belongs to a family of heavy fermions and thus we assume that the effective mass m^* of a quasiparticle is so great that it reaches from several hundreds to a thousand times as much as that of a bare electron m. The ratio of the effective mass of a quasiparticle to the mass of a bare electron m^*/m is proportional to the ratio of the Sommerfeld constant γ in the low temperature limit, since $\gamma = (\pi^2/3)(m^*k_F)k_B^2/2\pi^2\hbar^2$. The Sommerfeld constant γ of $CeCoIn_5$ in the low temperature limit is given as $\gamma \sim 1\ \mathrm{J\,K^{-2}\,mol^{-1}}$ under the magnetic field $H \sim 5$ T [20], which is consistent with the entropy balance argument at $H = 0$ T. Therefore, $m^*/m \sim 10^3$ as mentioned above. Then, we used $m^*/m = 400$, 500, and 600 as typical examples in figures 6–8. On the other hand, the effective Fermi energy E_F^* is estimated as follows. Using the lattice constants $a = 4.612$ Å and $c = 7.549$ Å [21], the Fermi energy of a non-interacting electron E_F in the 3d spherical model is estimated as $E_F = \hbar^2k_F^2/2m \sim 1.4 \times 10^4$ K. Thus, $E_F^* \sim (m/m^*) \times 1.4 \times 10^4$ K is 35 K, 28 K, and 24 K for $m^*/m = 400$, 500, and 600, respectively.

The factors $46/5(\mathrm{d}_{xy})$ and $4/5(\mathrm{d}_{x^2-y^2})$ in the right-hand side of equation (25) are numerical factors arising from the diagrams of the SC fluctuation correction of figures 4 and 5 for d_{xy} and $\mathrm{d}_{x^2-y^2}$ pairings. The difference of the numerical factors stems from the transformation property of the Cooper-pair wavefunctions $\phi_{xy}(\mathbf{k}) = 2\sin k_x \sin k_y$ and $\phi_{x^2-y^2}(\mathbf{k}) = \cos k_x - \cos k_y$ with respect to $\mathbf{k} \to \mathbf{k} + (\pi/a, \pi/a, 0)$. It can easily be seen from equation (25) that $\Pi_3(\mathbf{Q},0)/|\Pi_1(\mathbf{Q},0)|$ of the d_{xy} superconductor is about ten times larger than that of the $\mathrm{d}_{x^2-y^2}$ one. Moreover, we can see from figure 6 that in the vicinity of the absolute zero temperature, $\Pi_3(\mathbf{Q},0)/|\Pi_1(\mathbf{Q},0)|$ is linear in temperature with a monotonous increase as temperature decreases, due to the SC fluctuations as shown in figure 2.

Let us denote the solution of equation (23) with $y_0 = y_0^*$ by y^*. Namely, y_0^* by itself does not lead to the appearance of the AF-QCP. This can be immediately seen from the fact

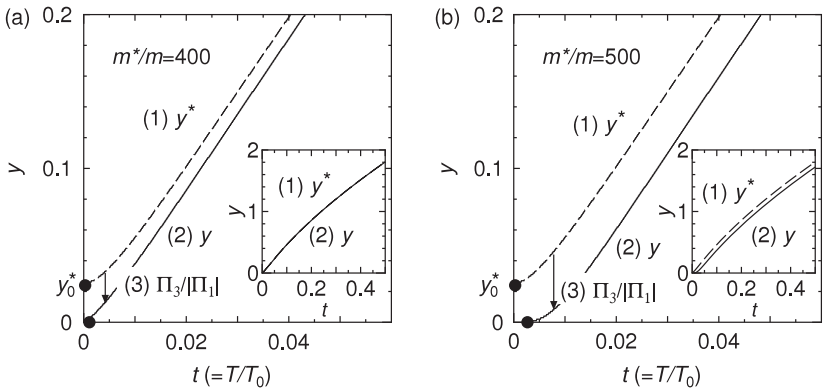

Figure 7. Temperature dependence of the deviation from the AF-QCP (a) for $m^*/m = 400$ and (b) for $m^*/m = 500$ where $h/E_F^* = 1/10$, $T_c = 0$ K, $H = 5.1$ T, and $y_1 = 1$ with a $d_{x^2-y^2}$ Cooper-pair wavefunction. The filled mark represents t_N, and $t_N = 5.0 \times 10^{-4}$ for (a) and $t_N = 2.3 \times 10^{-3}$ for (b). (1) y^*: the deviation from the AF-QCP (without the SC fluctuations). (2) y: the deviation from the AF-QCP (with the SC fluctuations). (3) $\Pi_3(\mathbf{Q}, 0)/|\Pi_1(\mathbf{Q}, 0)|$: the correction of the deviation from the AF-QCP due to the SC fluctuations.

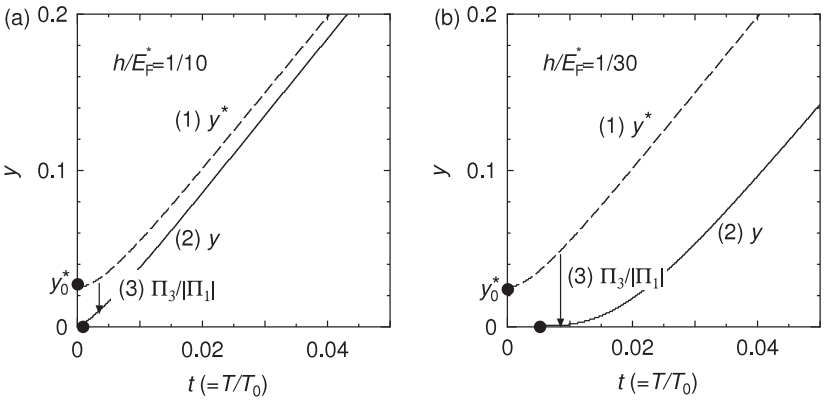

Figure 8. Temperature dependence of the deviation from the AF-QCP (a) for $h/E_F^* = 1/10$ and (b) for $h/E_F^* = 1/30$ where $m^*/m = 400$, $T_c = 0$ K, $H = 5.1$ T, and $y_1 = 1$ with a $d_{x^2-y^2}$ Cooper-pair wavefunction. The filled mark represents t_N, and $t_N = 5.0 \times 10^{-4}$ for (a) and $t_N = 6.0 \times 10^{-3}$ for (b). (1) y^*: the deviation from the AF-QCP (without the SC fluctuations). (2) y: the deviation from the AF-QCP (with the SC fluctuations). (3) $\Pi_3(\mathbf{Q}, 0)/|\Pi_1(\mathbf{Q}, 0)|$: the correction of the deviation from the AF-QCP due to the SC fluctuations.

that $y^* > 0$ over the entire region of temperature as shown in figures 7, 8. However, the additional involvement of $\Pi_3/|\Pi_1|$ as pertinent to the SC fluctuations gives rise to the appearance of the AF-QCP rather easily since $y_0^* \ll 1$ implies that $CeCoIn_5$ is located in a state which is not far from the AF state without the magnetic field. This is a fundamental reason why the SC fluctuations near H_{c2} promote the AF-QCP in the nearly AF metals.

Of course, in order to make the system arrive at the AF-QCP just at $T = 0$ and $H = H_{c2}(0)$, we need fine tuning of the parameters, such as the constant coupling g, the mass enhancement factor m^*/m, and the degree of deviation from the perfect nesting h. However, since we are interested in the gross T-dependence of the AF susceptibility $\chi_s(\mathbf{Q})$ from T_{c0} down to $T = 0$, the fine tuning of $y_0 = y(T = 0)$ is not so crucial to obtain NFL behavior of $\chi_s(\mathbf{Q}) \propto 1/y$ except in the narrow temperature region $T \ll T_{c0}$, as long as $|y_0| \ll 1$. This is a similar situation to where we were not concerned about whether the SC transition was a first-order transition or second-order one around $H = H_{c2}$ ($T \ll T_c$) as long as the first-order transition was a weak one.

The effective mass ratio m^*/m dependence of $\Pi_3/|\Pi_1|$ is shown in figure 6(a), which reveals that larger m^*/m leads to larger $\Pi_3/|\Pi_1|$. This behavior is attributed to the fact that $\Pi_3/|\Pi_1|$ is significantly affected by the SC fluctuations, which are larger as m^*/m becomes larger as shown in figure 2. Similarly, the energy scale for the deviation from the perfect nesting h dependence of $\Pi_3/|\Pi_1|$ is shown in figure 6(b), which reveals that $\Pi_3/|\Pi_1|$ is significantly affected by h in a manner in which smaller h leads to larger $\Pi_3/|\Pi_1|$. The reason is that $\Pi_3/|\Pi_1|$ contains the factor $[g/\max(T, h/2\pi)]^2$ on the right-hand side of equation (25) and it enables an inverse-T quadratic increase in $\Pi_3/|\Pi_1|$ with decreasing temperature in the region where $T > h/2\pi$, as mentioned above.

In conclusion, the novel coincidence of H_{QCP} and $H_{c2(0)}$ at $T = 0$ K is not accidental but essential and it owes much to the SC fluctuations. This is because the SC fluctuations are remarkable since they become one-dimensional near $H \simeq H_{c2(0)}$ owing to the Landau quantization of the Cooper-pair wavefunction. We have explained the relevance of the SC fluctuations to this novel coincidence by using the mode-coupling theory including the SC fluctuations. According to

this theoretical analysis, it becomes clear that the contribution of the SC fluctuations to the appearance of QCP greatly depends on the effective mass ratio m^*/m, the Cooper-pair wavefunctions ($d_{x^2-y^2}$ and d_{xy}), and the energy scale for deviation from the perfect nesting h. That is to say, the larger m^*/m and the smaller h, the larger the contribution of the SC fluctuations will be. Furthermore, the contribution of the SC fluctuations due to the d_{xy} superconductor is about ten times larger than that of the SC fluctuations due to the $d_{x^2-y^2}$ one.

Finally, it is noted that the field-induced QCP around H_{c2} proposed above is not unique to $CeCoIn_5$ but can be far more widespread. Namely, similar behavior is also observed both in $NpPd_5Al_2$ [22] and in $Tl_2Ba_2CuO_6$ [23].

References

[1] Paglione J, Tanatar M A, Hawthorn D G, Boaknin E, Hill R W, Ronning F, Sutherland M, Taillefer L, Petrovic C and Canfield P C 2003 *Phys. Rev. Lett.* **91** 246405

[2] Bianchi A, Movshovich R, Vekhter I, Pagliuso P G and Sarrao J L 2003 *Phys. Rev. Lett.* **91** 257001

[3] Bauer E D, Capan C, Ronning F, Movshovich R, Thompson D and Sarrao J L 2005 *Phys. Rev. Lett.* **94** 047001

[4] Miyake K 2007 *J. Phys.: Condens. Matter* **19** 125201

[5] Pham L D, Park T, Maquilon S, Thompson J D and Fisk Z 2006 *Phys. Rev. Lett.* **97** 056404

[6] Pagliuso P G, Movshovich R, Bianchi A D, Nicklas M, Moreno N O, Thompson J D, Hundley M F, Sarro J L and Fisk Z 2002 *Physica* B **312/313** 129

[7] Moriya T 1985 *Spin Fluctuations in Itinerant Electron Magnetism* (Berlin: Springer)

[8] Moriya T and Takimoto T 1995 *J. Phys. Soc. Japan* **64** 960

[9] Miyake K and Narikiyo O 1994 *J. Phys. Soc. Japan* **63** 3821

[10] Miyake K and Kuramoto Y 1991 *Physica* B **171** 20

[11] Kuramoto Y and Miyake K 1990 *J. Phys. Soc. Japan* **59** 2831

[12] Matsuda Y and Shimahara H 2007 *J. Phys. Soc. Japan* **76** 051005

[13] Larkin A I and Ovchinikov Y N 1965 *Sov. Phys.—JETP* **20** 762

[14] Fulde P and Ferrel R A 1964 *Phys. Rev.* **135** A550

[15] Movshovich R, Jaime M, Thompson J D, Petrovic C, Fisk Z, Pagliuso P G and Sarrao J L 2001 *Phys. Rev. Lett.* **86** 5152

[16] Tayama T, Harita A, Sakakibara T, Haga Y, Shishido H, Settai R and Onuki Y 2002 *Phys. Rev.* B **65** 180504

[17] Adachi H and Ikeda R 2003 *Phys. Rev.* B **68** 184510

[18] Bennemann K H and Ketterson J B 1989 *The Physics of Superconductors* vol I (Berlin: Springer)

[19] Moriya T, Takahashi Y and Ueda K 1995 *J. Phys. Soc. Japan* **59** 2905

[20] Petrovic C, Pagliuso P G, Hundley M F, Movshovich R, Sarrao J L, Thompson J D, Fisk Z and Monthoux P 2001 *J. Phys.: Condens. Matter* **13** L337

[21] Settai R, Shishido H, Ikeda S, Murakawa Y, Nakashima M, Aoki D, Haga Y, Harima H and Ōnuki Y 2001 *J. Phys.: Condens. Matter* **13** L627

[22] Aoki D, private communications

[23] Shibauchi T, private communications